Neuronal Mapping of the Heart with 6-[^{18}F]Fluorometaraminol[1]

Donald M. Wieland,* Karen C. Rosenspire, Gary D. Hutchins, Marcian Van Dort, Jill M. Rothley, Suresh G. Mislankar, Helen T. Lee,† Christopher C. Massin, David L. Gildersleeve, Philip S. Sherman, and Markus Schwaiger

Division of Nuclear Medicine, University of Michigan Medical Center, Ann Arbor, Michigan 48109-0552.
Received July 21, 1989

The false neurotransmitter metaraminol labeled with fluorine-18 has been used to noninvasively assess regional adrenergic nerve density in the canine heart. Intravenous administration of 6-[^{18}F]fluorometaraminol (FMR) results in high, selective accumulation of radioactivity in the heart; drug blocking studies with desipramine and reserpine confirm the neuronal locus of FMR. Iodine-125 labeled metaraminol, however, shows no selective accumulation in the canine heart. Positron emission tomography (PET) analyses with FMR of closed-chest dogs bearing left ventricular neuronal defects clearly delineate the region of neuronal impairment; blood perfusion in the left ventricle wall was homogeneous as determined by [^{13}N]NH_3 tomograms. The accumulation of FMR in regionally denervated dog heart correlates closely (r = 0.88) with endogenous norepinephrine concentrations. PET-generated ^{18}F time–activity curves demonstrate marked kinetic differences between normal and denervated myocardium. FMR/PET analysis could be used to assess the heterogeneity of sympathetic innervation in human heart disease contingent on the development of FMR with sufficiently high specific activity to clearly avoid pressor activity.

Tracer studies of the human heart using positron emission tomography (PET) have focused on the evaluation of blood flow and metabolic function.[2] The sympathetic nervous system of the heart, despite its alteration in a number of heart diseases, has been difficult to assess by noninvasive techniques.[3] This paper describes the successful use of 6-[^{18}F]fluorometaraminol (FMR) in neuronal mapping of the heart.

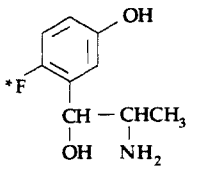

6-[^{18}F]FLUOROMETARAMINOL

Norepinephrine (NE) is the primary neurochemical transmitter of the sympathetic nervous system where it is localized predominantly in adrenergic nerve terminals. Endogenous NE tissue concentrations are generally accepted as quantitative indices of sympathetic nerve density. About 80% of NE in mammalian heart is synthesized in this organ, while 20% is derived from the circulating pool of NE.[4] Tissues with rich sympathetic innervation, such as the heart, also sequester large amounts of injected catecholamines.[5] Pharmacological blocking studies[6] and the combined use of autoradiographic and histochemical techniques[7] have demonstrated that [^{3}H]NE accumulates selectively in the adrenergic nerve endings of the heart. Metaraminol, a synthetic false neurotransmitter structurally similar to NE, has been employed extensively as an in vitro tool to study the NE uptake carrier.[8] Metaraminol not only shares the same neuronal uptake pathway as NE but utilizes the same storage and release pathways as well.[9] Earlier claims that metaraminol displaces NE from the peripheral nerve endings on a stoichiometric basis have been refuted; however, all studies to date support a neuronal locus for metaraminol.[10] This neuronal localization has led investigators to utilize [^{3}H]metaraminol as an index of adrenergic innervation in isolated tissue preparations of the rat[11] and rabbit.[12]

Two characteristics of metaraminol relative to NE make it attractive as a possible ^{18}F-labeled tracer for in vivo neuronal mapping by PET: (1) the pressor effect of metaraminol is only about $^1/_{20}$ that of NE;[13] (2) metaraminol has high metabolic stability since it is not a substrate for

Scheme I

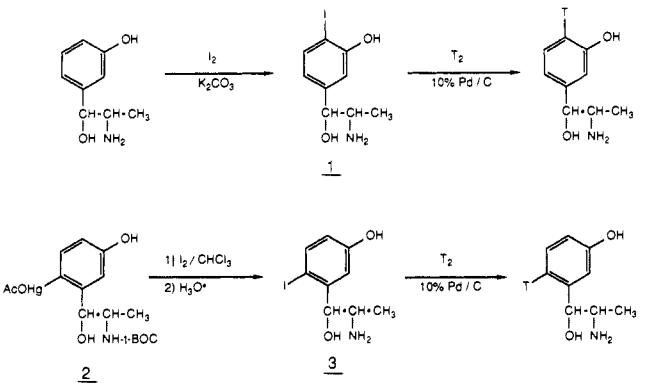

† Present address: Parke-Davis Pharmaceutical Research Division, Ann Arbor, MI.

(1) A preliminary report of this work has been presented: Hutchins, G. D.; Rothley, J. M.; Wieland, D. M.; Rosenspire, K. C.; Kuhl, D. E.; Schwaiger, M. Evaluation of 6-[F-18]-fluorometaraminol (FMR) kinetics in canine myocardium using positron emission tomography. Presented at the 35th Annual Meeting of the Society of Nuclear Medicine, San Francisco, CA, June 14–18, 1988 (Abstract in *J. Nucl. Med.* **1988**, *29*, 807).
(2) Schelbert, H. R.; Schwaiger, M. In *Positron Emission Tomography and Autogradiography. Principals and Applications for the Brain and Heart*; Phelps, M. E., Mazziotta, J. C., Schelbert, H. R., Eds.; Raven Press: New York, 1986; pp 581–661.
(3) Sisson, J. C.; Lynch, J. P.; Johnson, J.; Jaques, S.; Wu, D.; Bolgos, G.; Lucchesi, B. R.; Wieland, D. M. *Am. Heart J.* **1988**, *116*, 67.
(4) Kopin, T. J.; Gordon, E. K. *Nature* **1963**, *199*, 1289.
(5) (a) Whitby, L. G.; Axelrod, J.; Weil-Malherbe, H. *J. Pharmacol. Exp. Ther.* **1961**, *132*, 193. (b) Axelrod, J.; Weil-Malherbe, H.; Tomchick, R. *J. Pharmacol. Exp. Ther.* **1959**, *127*, 251. (c) Crout, J. R. *Arch. Exp. Pathol. Pharmacol.* **1964**, *248*, 85. (d) Wieland, D. M.; Brown, L. E.; Rogers, W. L.; Worthington, K. C.; Wu, J.-L.; Clinthorne, N. H.; Otto, C. A.; Swanson, D. P.; Beierwaltes, W. H. *J. Nucl. Med.* **1981**, *22*, 22.
(6) (a) Hertting, G.; Axelrod, J.; Whitby, L. G. *J. Pharmacol. Exp. Ther.* **1961**, *134*, 146. (b) Burgen, A. S. V.; Iversen, L. L. *Br. J. Pharmacol.* **1965**, *25*, 34.
(7) Iversen, L. L. In *Uptake Processes For Biogenic Amines*; Iversen, L. L., Iversen, S. D., Snyder, S. H., Eds.; Plenum Press: New York, 1975; p 381.
(8) Ross, S. B. In *The Mechanisms of Neuronal and Extraneuronal Transport of Catecholamines*; Paton, D. M., Ed.; Raven: New York, 1976; p 67.

0022-2623/90/1833-0956$02.50/0

Table I. Tissue Concentrations of [^{3}H]Metaraminol (MR) and [^{3}H]Norepinephrine (NE) in Dog

	^{3}H concentration, % kg dose/g ± SEM[a-c]					
	0.5 h			24 h		
tissue	[^{3}H]NE	[6-^{3}H]MR	[4-^{3}H]MR	[^{3}H]NE	[6-^{3}H]MR	[4-^{3}H]MR
heart[d]	0.74 ± 0.03	0.72 ± 0.01	0.55 ± 0.05	0.16 ± 0.04	0.51 ± 0.15	0.59 ± 0.05
blood	0.04 ± 0.01	0.03 ± 0.01	0.03 ± 0.01	0.017 ± 0.001	0.009 ± 0.003	0.008 ± 0.004
lung	0.18 ± 0.03	0.13 ± 0.01	0.20 ± 0.01	0.03 ± 0.01	0.05 ± 0.01	0.03 ± 0.01
liver	0.27 ± 0.01	0.42 ± 0.09	0.42 ± 0.18	0.09 ± 0.01	0.17 ± 0.05	0.13 ± 0.06
spleen	0.81 ± 0.11	0.88 ± 0.14	0.81 ± 0.16	0.52 ± 0.10	0.73 ± 0.16	0.50 ± 0.28
H/B[e]	19	24	18	9	57	74

[a] $N = 3$ per time interval for [6-^{3}H]MR; $N = 2$ per time interval for [^{3}H]NE and [4-^{3}H]MR. [b] Specific activities were ([^{3}H]NE) 14 Ci/mmol, ([6-^{3}H]MR) 21 Ci/mmol, and ([4-^{3}H]MR) 19.5 Ci/mmol. [c] Female mongrel dogs weighing 14–22 kg were used; 100 μCi of tracer was injected iv bolus. [d] Wall of left ventricle. [e] Left ventricle to blood concentration ratio.

Table II. Neuronal Selectivity of [^{3}H]NE and [^{3}H]MR in Rat Tissues[a,b]

	concentration, % dose/g ± SEM[c]					
	Lt atrium	Rt atrium	Lt ventricle	Rt ventricle	spleen	blood
	[^{3}H]Norepinephrine					
control (N = 5)	4.75 ± 0.28	4.86 ± 0.68	4.10 ± 0.23	4.86 ± 0.24	0.85 ± 0.110	0.065 ± 0.005
6-hydroxydopamine ($N = 5$)	0.39 ± 0.10	0.29 ± 0.06	0.60 ± 0.22	0.41 ± 0.07	0.25 ± 0.05	0.052 ± 0.013
change[d]	−92%	−94%	−85%	−92%	−71%	−20%
	[^{3}H]Metaraminol					
control ($N = 7$)	5.26 ± 0.43	5.19 ± 0.14	5.38 ± 0.39	6.10 ± 0.45	1.88 ± 0.25	0.062 ± 0.012
6-hydroxydopamine ($N = 7$)	0.75 ± 0.24	0.86 ± 0.33	1.05 ± 0.27	1.32 ± 0.45	0.46 ± 0.13	0.158 ± 0.051
change[d]	−86%	−83%	−86%	−80%	−76%	+155%

[a] Treated rats received 100 mg/kg (ip) of 6-hydroxydopamine hydrobromide 5 days prior to 25 μCi tracer iv injection; this treatment has been shown previously in our laboratory to lower endogenous NE levels in the left ventricle by 90% (ref 35). Tracer specific activities were the same as in Table I. [^{3}H]MR represents [6-^{3}H]metaraminol. All animals were sacrificed 90 min after tracer injection. [b] When thallium-201 (23–28 μCi) was used as a blood perfusion tracer in this same protocol ($N = 6$), changes in the radioactivity levels in the four heart regions ranged from 0 to +7%. [c] Concentrations are given in % dose/g normalized to a 200-g rat. Rats (female Sprague–Dawley) weighed 168–210 g. [d] $p < 0.001$ for all tissue concentration changes except blood, which was not significant.

either monoamine oxidase or catechol-*O*-methyltransferase.[14] The lower pressor activity of metaraminol makes it more compatible with the relatively low specific activities (1–15 Ci/mmol) achievable by ^{18}F electrophilic fluorination,[15] and the high metabolic stability of metaraminol will simplify tracer kinetic analysis. The above rationale prompted our recent regiospecific synthesis and preliminary biological evaluation of FMR.[16] The present work (1) demonstrates that [^{3}H]metaraminol faithfully labels the storage pool of norepinephrine in vivo, (2) confirms that FMR is also a marker for sympathetic storage vesicles, and (3) validates FMR as an in vivo neuronal marker in the regionally denervated dog heart.

Chemistry

Scheme I illustrates the procedure used for the synthesis of [4-^{3}H]metaraminol and [6-^{3}H]metaraminol. The intermediate 4-iodometaraminol (**1**) was obtained by direct iodination of metaraminol. A more circuitous route, requiring the 6-HgOAc derivative **2**,[16] was employed in the regiospecific synthesis of 6-iodometaraminol (**3**). Tritium labeling was performed in a commercial laboratory by catalytic reduction of the iodometaraminols with 10 Ci of tritium gas. Racemization at the benzylic position, if it occurred, would result in diastereomeric conversion from the *R,S* to the *S,S* configuration (erythro → threo), thus permitting detection by nonchiral techniques. Evidence for the retention of the 1*R*,2*S* configuration during the reaction sequence is based on comparison of the UV/radio-HPLC behavior of [^{3}H]metaraminol with that of a diastereomeric mixture obtained by partially racemizing unlabeled metaraminol in refluxing 6 N HCl for 7 days. ^{1}H NMR and optical rotation measurements of unlabeled metaraminol, obtained by modification of Scheme I in which hydrogen gas was substituted for tritium gas, also confirm retention of the 1*R*,2*S* configuration. ^{1}H NMR of metaraminol and its acid-induced diastereomer have been reported.[17] Although the regiospecificity of tritium incorporation in the 4- and 6-position, respectively, of metaraminol was not confirmed by ^{3}H NMR, reductive tritiodehalogenation of similar phenolamines such as octopamine is known to give regiospecific incorporation.[18]

Fluorine-18 labeling of metaraminol was achieved by fluorodemercuration of **2** with acetyl hypo[^{18}F]fluorite as previously described.[16] Labeling of metaraminol with iodine-125 was performed by direct iodination using the chloramine-T method followed by either C-18 Sep-Pak or reversed-phase HPLC separation of the 4- and 6-[^{125}I]iodo isomers.

(9) Crout, J. R.; Alpers, H. S.; Tatum, E. L.; Shore, P. A. *Science* **1964**, *145*, 828.
(10) Anton, A. H.; Berk, A. I. *Eur. J. Pharmacol.* **1977**, *44*, 161.
(11) Hermann, W.; Graefe, K-H. *Naunyn-Schmiedeberg's Arch. Pharmacol.* **1977**, *296*, 99.
(12) Duckles, S. P. *Eur. J. Pharmacol.* **1980**, *67*, 355.
(13) Crout, J. R. *Circ. Res. Suppl. I* **1966**, *18* and *19*, I-120.
(14) Fuller, R. W.; Snoddy, H. D.; Perry, K. W.; Bernstein, J. R.; Murphy, P. J. *Biochem. Pharmacol.* **1981**, *30*, 2831.
(15) (a) Blessing, G.; Coenen, H. H.; Franken, K.; Qaim, S. M. *Appl. Radiat. Isot.* **1986**, *37*, 1135. (b) Nickles, R. J.; Gatley, S. J.; Votaw, J. R.; Kornguth, M. L. *Appl. Radiat. Isot.* **1986**, *37*, 649.
(16) Mislankar, S. G.; Gildersleeve, D. L.; Wieland, D. M.; Massin, C. C.; Mulholland, G. K.; Toorongian, S. A. *J. Med. Chem.* **1988**, *31*, 362.
(17) Saari, W. S.; Raab, W. A.; Engelhardt, E. L. *J. Med. Chem.* **1968**, *11*, 1115.
(18) Bloxsidge, J. P.; Elvidge, J. A.; Gower, M.; Junes, J. R.; Evans, E. A.; Kitcher, J. P.; Warrell, D. C. *J. Labelled Cmpds. Radiopharm.* **1981**, *18*, 1141.

Table III. Tissue Concentrations of 4-[^{125}I]Iodometaraminol and 6-[^{125}I]Iodometaraminol in Dog[a,b]

	^{125}I concentration, % kg dose/g			^{125}I concentration, % kg dose/g	
tissue	4-iodo	6-iodo	tissue	4-iodo	6-iodo
heart (LV)	0.17	0.05	spleen	0.26	0.08
blood	0.04	0.05	thyroid	0.20	0.06
lung	0.25	0.26	adrenal medulla	0.45	0.20
liver	0.50	0.49	H/B[c]	4	1

[a] Female mongrel dogs (N = 1) were sacrificed 30 min after iv tracer injection; the tracers were carrier-free. [b] The dog receiving 4-[^{125}I]iodometaraminol (75 μCi) weighed 15.9 kg; the 6-[^{125}I]iodometaraminol (55 μCi) dog weighed 13.3 kg. [c] Left ventricle to blood concentration ratio.

Biological Results

The concentration of radioactivity in selected tissues of the dog following intravenous injection of [6-^{3}H]-metaraminol, [4-^{3}H]metaraminol, and [^{3}H]norepinephrine are compared in Table I. The two tritium-labeled metaraminols displayed very similar whole-body distributions in the dog at 0.5 and 24 h postinjection, which strongly suggests that extensive hydroxylation in the 4-position is not occurring. Similar results have been obtained in rats (data not shown). The distribution of the [^{3}H]-metaraminols in dogs is nearly identical with that obtained for [^{3}H]norepinephrine at 0.5 h. Organs with rich sympathetic innervation such as heart and spleen show the highest concentration of tracer. Retention of tracer in the heart and spleen at 24 h was more pronounced with the [^{3}H]metaraminols than with [^{3}H]norepinephrine, a finding consistent with the greater metabolic stability of metaraminol.

The percent radioactivity in a tissue that is localized within the sympathetic nerves—the neuronal selectivity—was also very similar for [^{3}H]norepinephrine and [^{3}H]metaraminol in the heart and spleen as shown in Table II. The neuronal selectivity was determined in chemically sympathectomized rats in which destruction of the peripheral sympathetic nerves was accomplished by intravenous injection of the neurotoxin 6-hydroxydopamine (6-OHDA). The most important tissue from a nuclear imaging standpoint is the thick-walled left ventricle; in this tissue the neuronal selectivity was 85% and 86% for [^{3}H]norepinephrine and [^{3}H]metaraminol, respectively. To ascertain whether cardiac blood flow was greatly altered in these 6-OHDA treated animals, thallium-201, a blood perfusion agent, was administered by using the same protocol. Percent changes in thallium-201 concentrations in the heart of sympathectomized rats versus control animals ranged from 0% to +7%.

The distributions of 4- and 6-[^{125}I]iodometaraminol in selected tissues of the dog are given in Table III. Accumulation of these tracers in the heart was nearly 1 order of magnitude less than was observed with the parent ^{3}H-labeled metaraminols (Table I). Heart tissue concentrations of the radioiodinated metaraminols were so low in rats (data not shown) that sympathectomy studies with 6-OHDA were deemed impractical.

The time course of distribution of FMR in the heart and three other tissues after iv injection in the rat is shown in Figure 1. The uptake in the heart is rapid, high, and essentially irreversible over the 4-h study. The slow efflux of FMR from the heart is in agreement with the 2–3 day half-life of unlabeled metaraminol in the rat heart reported by Shore and co-workers.[25] The lung, liver, and especially blood are the greatest sources of interfering radioactivity in cardiac scintigraphy. The heart to blood concentration

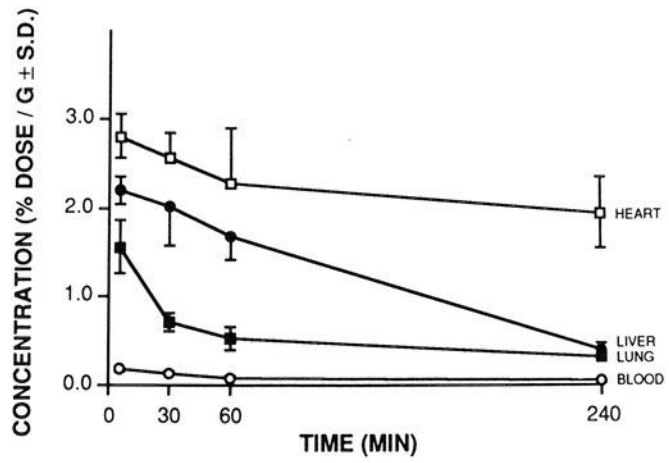

Figure 1. Temporal pattern of distribution of FMR in the rat. Two males and three females were sacrificed per time point. Concentrations are normalized to a 200-g rat. Although rat weights ranged from 182 to 335 g, the majority weighed approximately 200 g. The rats sacrificed at 240 min received 46–50 μCi of tracer by iv injection; all other rats received 25–27 μCi. Heart tissue samples were from the left ventricle.

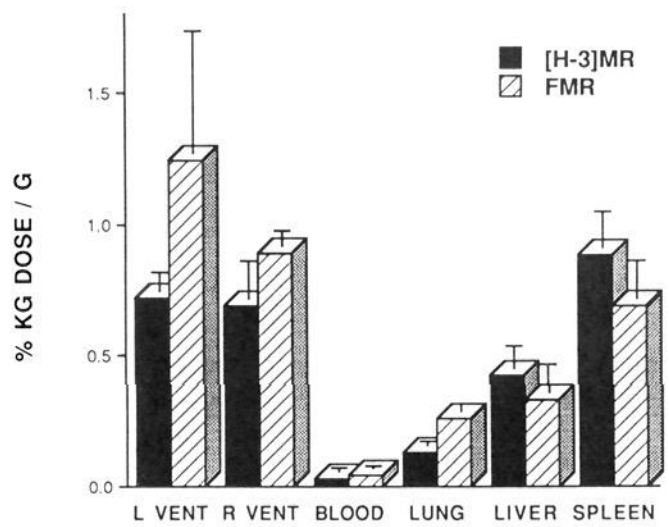

Figure 2. Comparative tissue distribution of [6-^{3}H]metaraminol and FMR in selected tissues of the dog at 60 and 30 min, respectively. Concentrations are given in % kg dose/g ± SD; N = 3 for [6-^{3}H]metaraminol and N = 4 for FMR.

Table IV. Tissue Concentrations of FMR in Dogs[a]

tissue	^{18}F concentration, % kg dose/g ± SD	tissue	^{18}F concentration, % kg dose/g ± SD
left ventricle	1.24 ± 0.47	spleen	0.69 ± 0.14
right ventricle	0.89 ± 0.06	muscle[b]	0.07 ± 0.03
left atrium	1.54 ± 0.20	pancreas[b]	0.60 ± 0.30
right atrium	1.44 ± 0.59	kidney[b]	0.41 ± 0.01
lung	0.26 ± 0.03	adrenal cortex	0.59 ± 0.13
liver	0.33 ± 0.11	adrenal medulla	9.89 ± 2.65
blood	0.04 ± 0.01		

[a] N = 4; animals were two female (15.0 and 18.6 kg) and two male (20.4 and 21.0 kg) mongrel dogs. Radiotracer injections were given iv bolus; animals were killed 1 h following radiotracer injection. The female dogs were each administered 0.45 mCi; male dogs were administered 2.0 mCi each. [b] N = 2.

ratio of 16.5 at 5 min increases to nearly 50 at 4 h. The overall tissue distribution pattern of FMR in the dog (see Table IV) closely parallels that observed in rats. Figure 2 emphasizes the similarities in the distributions of [^{3}H]metaraminol and FMR in canine tissues. Like [^{3}H]-metaraminol itself, FMR avidly accumulates in NE-rich tissues, in particular the walls of the four chambers of the heart and the adrenal medulla. Left ventricle to blood and left ventricle to lung concentration ratios of 30 and 5, respectively, were obtained 1 h post iv injection of FMR; respective values of 24 and 5 were obtained with [6-^{3}H]MR at 30 min.

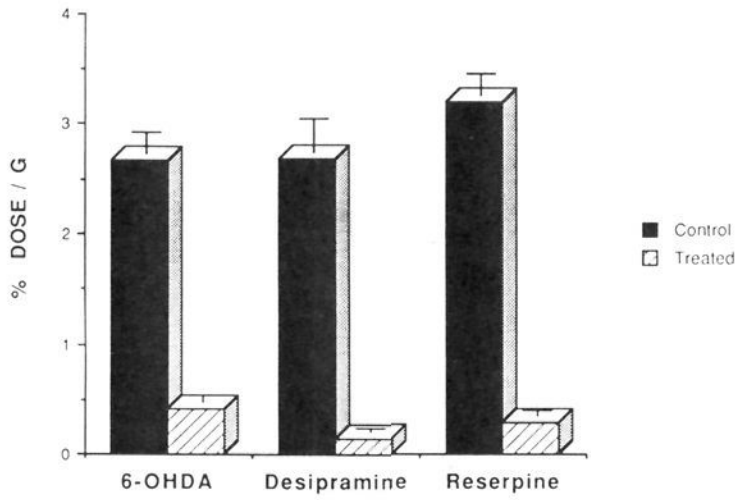

Figure 3. The effect of drugs on the concentration of FMR in the rat left ventricle. Drug-treated animals showed the following decreases in left ventricular activity: 6-OHDA, −84%; desipramine, −94%; reserpine, −91%. Similar decreases in radioactivity accumulation were observed when [^{3}H]norepinephrine was used as tracer: 6-OHDA, −85%; desipramine, −97%; reserpine, −98%. Rats were pretreated with 6-OHDA, desipramine, or reserpine followed by intravenous injection of 5–10 μCi of FMR. Concentrations are given in % dose/g ± SD normalized to a 250-g rat. Results are the means of six, four, and six rats in both control and treated animals in each of the three drug groups, respectively. 6-OHDA·HBr (100 mg/kg, ip) was administered 5 days prior to tracer injection. Desipramine-HCl (10 mg/kg ip) was given 30 min prior to tracer injection and reserpine (1 mg/kg ip) 3 h prior to tracer injection. All animals were sacrificed 90 min after tracer administration.

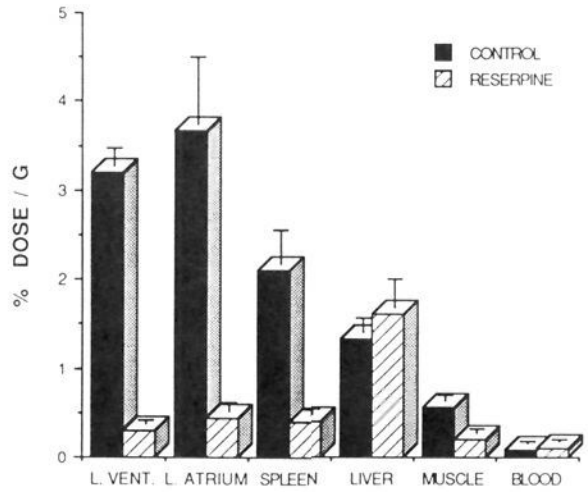

Figure 4. The effect of reserpine pretreatment on the concentration of FMR in selected tissues of the rat. Concentrations are given in % dose/g ± SD normalized to a 250-g rat (N = 6 per group). Reserpine (1 mg/kg ip) was given 3 h prior to tracer injection. Animals were sacrificed 90 min after tracer administration.

Pharmacological studies, summarized in Figure 3, strongly support a neuronal locus for FMR. Chemical sympathectomy with 6-OHDA or pretreatment with the neuronal uptake-1 blocker desipramine greatly diminishes FMR accumulation in the left ventricle. The similar effect of reserpine, a specific inhibitor of the vesicular uptake carrier protein, suggests that a substantial portion of FMR is sequestered within intraneuronal storage granules of the heart. The locus of action of desipramine and reserpine in the adrenergic nerve ending is depicted in Scheme II. Reserpine blockade of tracer sequestration extends to other adrenergic-rich tissues such as left atrium and spleen as shown in Figure 4. It is noteworthy that liver and blood radioactivity levels actually increase in response to reserpine pretreatment—likely a result of diminished tracer uptake in the sympathetic nerves.

PET Imaging Results

This work was aimed at validating FMR as an in vivo neuronal marker by using the phenol-denervated dog heart

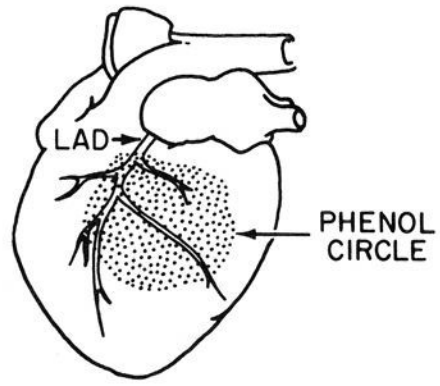

Figure 5. Schematic depicting the application of phenol (88% solution in ethanol, v/v) to the epicardial surface of the anterior wall of the dog heart. LAD is the left anterior decending artery.

Scheme II

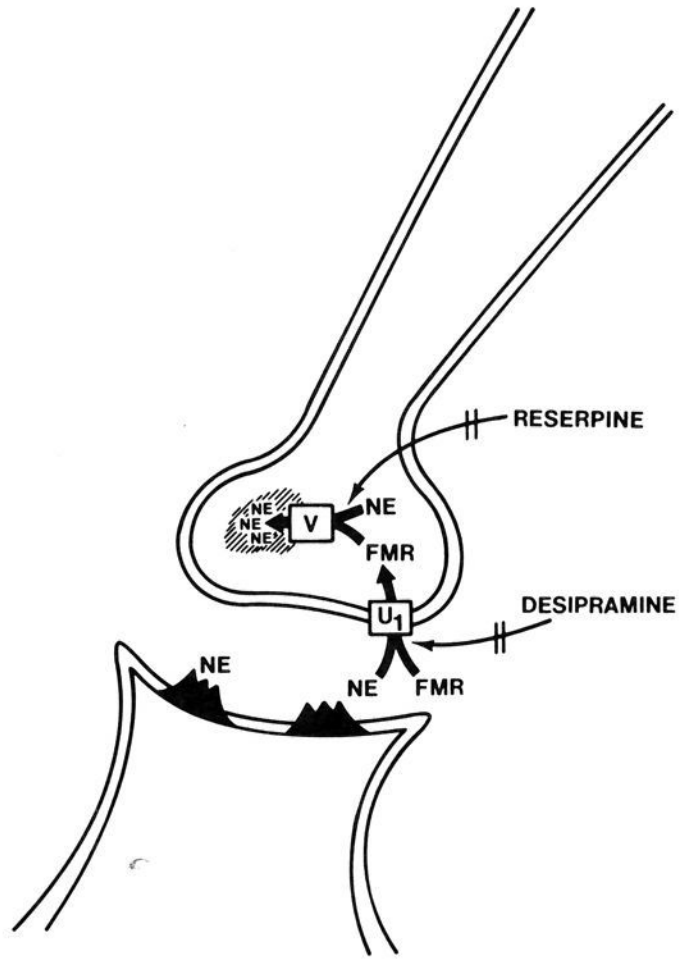

model depicted in Figure 5. Histochemical fluorescence studies of the normal heart have shown that sympathetic nerve fibers pass through the subepicardium along the coronary arteries.[19] The topical application of phenol to the epicardium has become an established technique for selectively destroying sympathetic fibers in discrete areas of the heart; vagal innervation is unaffected.[20] Tissue damage, as determined by histologic examination, extends to a depth of only 0.25 mm.[21] Scintigraphic studies with thallium-201 have demonstrated the patency of myocardial blood flow in the phenol-lesioned dog heart.[3]

To define the relationship between blood flow and regional FMR uptake, PET studies with the blood perfusion tracer [^{13}N]NH_3 were included in these imaging experiments. The acquisition of dynamic imaging data was initiated at the time of injection and continued either 20 min

(19) Randall, W. C. In *Neural Regulation of The Heart*; Randall, W. C., Ed.; Oxford University Press: New York, 1977; p 45.
(20) (a) Martins, J. B.; Zipes, D. P. *Circ. Res.* **1980**, *47*, 33. (b) Inoue, H.; Zipes, D. P. *Circulation* **1987**, *75*, 877. (c) Barber, M. J.; Mueller, T. M.; Davies, B. G.; Zipes, D. P. *Circ. Res.* **1984**, *55*, 532. (d) Chilian, W. M.; Boatwright, R. B.; Shoji, T.; Griggs, D. M., Jr. *Circ. Res.* **1981**, *49*, 866. Kaye, M. P.; Randall, W. C. *Cardiovasc. Res.* **1970**, *5*, 154.
(21) Kaye, M. P.; Brynjolfsson, G. G.; Geis, W. P. *Cardiologia* **1968**, *53*, 139.

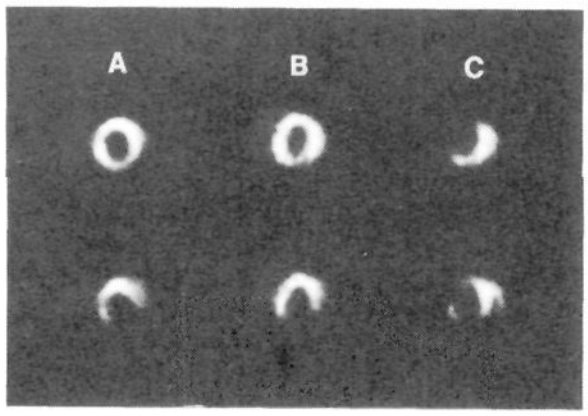

Figure 6. PET images of the canine heart. Panel A shows the distribution of ^{18}F in two contiguous slices of the mid-left ventricle of a normal dog (female, 19.6 kg) 40 min after iv injection of FMR. Panels B and C show the distribution of ^{13}N and ^{18}F, respectively, following the sequential iv injection of $[^{13}N]NH_3$ and FMR in a phenol-treated dog. The $[^{13}N]NH_3$ images were obtained 10 min after tracer injection; the FMR images were obtained 40 min after injection. The study shown in panels B and C was performed 4 days following the painting of the epicardial surface of the left anterior wall of the left ventricle in the region of the LAD with an 88% solution of phenol in ethanol (v/v). The marked reduction in FMR retention in the anterior wall of the left ventricle (panel C) following this denervation procedures is in sharp contrast to the well-preserved blood flow in this region as demonstrated by the $[^{13}N]NH_3$ images (panel B). These results demonstrate the ability of FMR and PET to detect areas of regional denervation in the canine myocardium. Images in B and C are from a 14-kg male dog anesthetized with sodium pentobarbital (30 mg/kg). The injected dose of $[^{13}N]NH_3$ was 4.4 mCi; the dose of FMR was 1.1 mCi. Specific activity of $[^{13}N]NH_3$ was 200–400 Ci/mmol; FMR specific activity was 3.8 Ci/mmol.

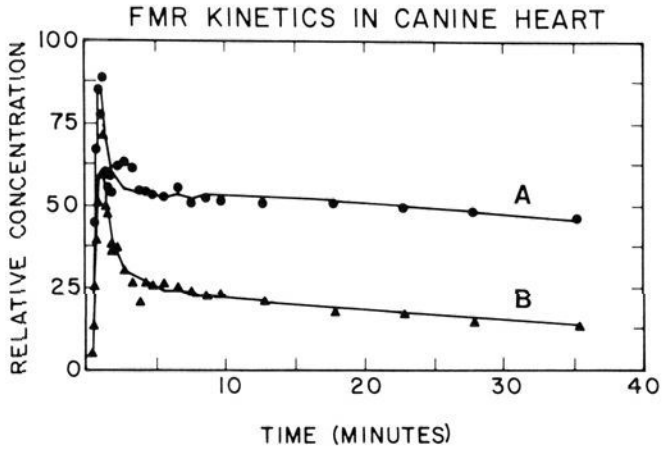

Figure 7. The kinetics of FMR in the phenol-lesioned dog heart in normal (A) and regionally denervated myocardium (B). The initial peak of myocardial radioactivity in each curve represents the spillover of counts from left ventricular blood into the myocardium due to a partial volume distortion created by the low resolution of the PET scanner. The fast component of tracer efflux represents diffusion of extracellular FMR from tissue to capillary blood; the slow component represents the neuronal release of FMR. The amplitude of the slow washout component is markedly reduced in the denervated tissue, indicating the inability of the neurons to retain FMR.

or 40 min for $[^{13}N]NH_3$ and FMR, respectively. Figure 6 shows corresponding cross sectional images of the heart obtained following FMR or $[^{13}N]NH_3$ injection. Blood flow was homogeneous throughout the myocardium in the phenol-painted dogs as evidence by the normal $[^{13}N]NH_3$ images; however, FMR uptake was markedly decreased in the anterior septal aspects of the left ventricle. Regional time-^{18}F activity curves (see Figure 7) derived from phenol-lesioned and nonlesioned myocardial areas reveal rapid and high initial uptake of FMR in both areas followed by a pronounced efflux of tracer from the denervated area.

To confirm that FMR maps regions of sympathetic denervation, the phenol-treated dogs were sacrificed following the imaging experiments, and their hearts were

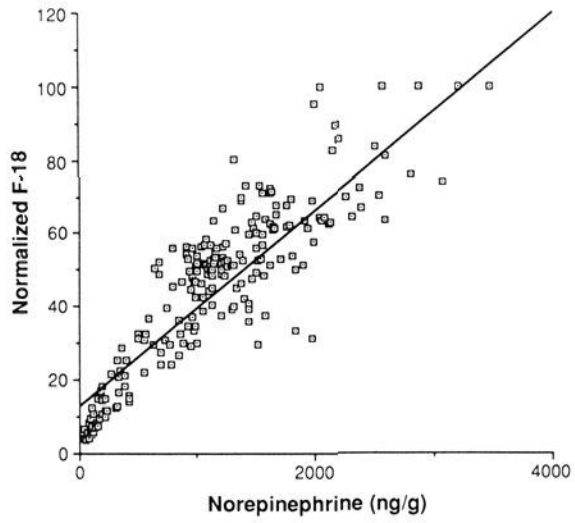

Figure 8. Correlation of FMR versus endogenous NE in the phenol-treated dog heart. Four to seven days post surgery and 1 h after iv FMR administration, five phenol-treated dogs were sacrificed by pentobarbital/KCl overdose. The hearts were rapidly excised, blotted and sliced into four approximately 1 cm thick transverse slices through the left ventricle from the apex to the atrioventricular groove. Each slice was quickly cut into 4–12 radial segments, weighed, and counted for radioactivity in a chilled counter. Representative samples were also taken from the left and right atria and right ventricle. After freezing, each sample was minced and homogenized in 9 volumes of cold 0.4 M perchloric acid and centrifuged (12000*g*; 15 min; 5 °C). The supernatants were than analyzed for endogenous NE levels using HPLC with fluorescence detection.[30] The graph shows the relationship between endogenous NE concentrations and FMR levels expressed in % kg dose/g values (i.e., the concentration of radioactivity as percent of the injected dose in a gram of tissue normalized to a 1-kg body weight). To correct for interanimal variations, the % kg dose/g ± SD values were normalized so that the segment with the highest concentration of fluorine-18 activity (i.e., atria) represents 100%.

removed and counted for fluorine-18 and analyzed for endogenous NE. Figure 8 presents the relationship between FMR levels and endogenous NE concentrations in 210 heart tissue samples from five phenol-treated dogs. A correlation coefficient of 0.88 was observed between the two measurements. In maximally denervated segments removed from the anterior wall of the left ventricle, NE and FMR levels decreased 80 ± 16% and 70 ± 18%, respectively, compared to diametrically opposed segments excised from the posterior wall of the left ventricle (Table V). The respective segments excised from control dogs showed NE and FMR differences of less than 5%.

Discussion

Abnormalities in the adrenergic nervous system of the heart are thought to be involved in clinical disorders such as congestive heart failure, myocardial ischemia and infarction. Imbalances in innervation of the heart may cause arrhythmias and sudden death.[22,23] The work presented here (1) describes our initial studies with $[^{3}H]$metaraminol, which illustrate the ability of this tracer to serve as a selective in vivo marker for the adrenergic neurons of the heart; (2) demonstrates that radioiodine labeling of metaraminol destroys its selective affinity for heart tissue; and (3) shows that labeling metaraminol with the positron-emitting radioisotope fluorine-18 produces a highly selective neuronal tracer (FMR) that can be used to ex-

(22) Manger, W. M. In *Catecholamines in Normal and Abnormal Cardiac Function*; Manger, W. M., Ed.; Harper Press: New York, 1982.
(23) (a) Patterson, E.; Holland, K.; Eller, B. T.; Lucchesi, B. R. *Am. J. Cardiol.* **1982**, *50*, 1414. (b) Muntz, K. H.; Hagler, H. K.; Boulas, H. J.; Willerson, J. T.; Buja, L. M. *Am. J. Pathol.* **1984**, *114*, 64.

Table V. FMR and Endogenous NE Concentrations from Midbasal Slices of Phenol-Treated Canine Myocardium

	NE, ng/g ± SD		normalized FMR, % kg dose/g ± SD[a]	
	anterior wall	posterior wall	anterior wall	posterior wall
control (N = 3)	1657.6 ± 444.4[b]	1611.8 ± 609.8	63.6 ± 11.6[b]	64.9 ± 17.5
phenol treated (N = 5)[d]	303.4 ± 337.4[c]	1464.8 ± 380.4	14.5 ± 10.6[c]	53.8 ± 14.2

[a] See legend to Figure 5 for method of normalization. [b] No significant difference compared to posterior wall with the Student's t-test. [c] $p < 0.001$ compared to posterior wall of control and phenol-treated dogs. [d] In each of 5 phenol-treated dogs, the three lowest contiguous values for NE and FMR concentrations in each of the two midbasal slices (a total of six segments/dog) were averaged to represent the concentration in the area affected by phenol. The segments were from the anterior wall; common borders were shared among the segments from both slices. For comparison, three posterior wall segments which were diametrically opposed to the lowest values in each of the two slices were averaged to represent "normal" myocardium. In each of three control (sham-treated) dogs, NE and FMR values were averaged from three adjacent regions of the anterior wall in each of the two midbasal slices. These values were then compared to values in diametrically opposed segments to determine the variability within control animals.

ternally visualize regional neuronal defects of the heart.

The diminished accumulation of radioiodinated metaraminol in adrenergically innervated tissues such as heart, spleen, and adrenal medulla is consistent with similar studies of tyramine[24] and dopamine.[25] On the basis of the low thyroid radioactivity levels that were observed with the ^{125}I-labeled tracers (Table III), in vivo deiodination was not a contributing factor. The lower retention in neuronal-rich tissue may be due to either decreased active transport through the neuronal cell membrane or to impaired entrapment within the catecholamine storage vesicles. Although structural requirements for neuronal uptake[8] and subsequent neuronal accumulation[26] are not stringent, it is perhaps not surprising that introduction of a large substituent such as iodine into a small sympathomimetic amine such as metaraminol would decrease its neuroaffinity. These findings, in fact, serve to highlight the importance of fluorine-18 as a biomimetic radiosubstituent in tracer design.

The use of FMR with PET is to our knowledge the first potentially quantitative technique available for probing the functional status of cardiac adrenergic nerves in vivo. FMR traces specifically the transport of NE into the neuron and its subsequent uptake and sequestration in the intraneuronal storage vesicles. The ability of FMR to share these energy-requiring transport processes, which give rise to its highly selective accumulation in heart tissue, should make it an ideal radiopharmaceutical for assessing neuronal abnormalities of the heart. The cellular and subcellular kinetics of FMR have yet to be determined; however, the kinetic constants for metaraminol transport by the uptake-1 carrier are nearly identical with those for norepinephrine.[8] Fluorocatecholamines at the tracer level are known to mimic their parent amines in vivo.[27] The results of the vesicular blocking studies with [^{3}H]-metaraminol and FMR are consistent with the work of Shore and co-workers who observed similar in vivo blockade of metaraminol binding to the heart of reserpinized rats.[28]

The concentration of FMR in the regionally denervated dog heart correlated closely with tissue NE content (Figure 8). However, the pattern of FMR retention serves more as a comparative index of the functional integrity of the neurons in various heart regions rather than as a quantitative map of heart NE levels. The amount of radiolabeled NE taken up by various tissues following intravenous injection depends on both the density of sympathetic innervation and regional differences in blood flow.[7,29] It should be noted that endogenous NE content may not be the best index of adrenergic nerve density in all models of neuronal alteration. For instance, in the surgically denervated dog heart, it has been shown that [^{3}H]NE heart concentrations are a better index of the reinnervation process than tissue NE content.[30] This may derive from the possibility that a tracer such as [^{3}H]NE, and likely FMR as well, map a different facet of neuronal function than that represented by the endogenous NE pattern. Tissue NE represents a composite picture of the ability of the neuron to synthesize and store NE as well as to sequester NE through the reuptake process; [^{3}H]NE or FMR tissue content reflect only the neuron's ability to take up and store NE.

The radiolabeled guanethidine analogue *meta*-[^{123}I]-iodobenzylguanidine has been used with single photon emission tomography (SPECT) to study the neuronal integrity of the heart.[3,31] The inherent sensitivity limitations of SPECT will likely restrict this approach to qualitative assessment of relatively large areas of myocardial denervation. In contrast to currently used SPECT instrumentation systems, which provide image resolutions in the range of approximately 18–20 mm at FWHM, state-of-the-art PET scanners produce heart images with a resolution of 6–10 mm. Ischemic heart disease may cause regional abnormalities in neuronal function and the resulting heterogeneity of sympathetic innervation may predispose patients to cardiac arrest.[20b,23] Thus an emphasis should be placed on developing a noninvasive technique sufficiently sensitive to detect small areas of neuronal loss that may accompany perfusion abnormalities in the human heart.

Although FMR should not be a substrate for catechol-*O*-methyltransferase or monoamine oxidase, studies have been carried out to determine the extent to which FMR is metabolized in vivo and whether these metabolites are localized in heart. Uptake of labeled metabolites by the heart would hamper tracer kinetic modeling approaches which assume uptake and efflux of only FMR from the neuronal compartment of the heart. In a detailed meta-

(24) Counsell, R. E.; Smith, T. D.; Ranade, V. V.; Noronha, O. P. D.; Desai, P. *J. Med. Chem.* **1973**, *16*, 684.
(25) Fowler, J. S.; MacGregor, R. R.; Wolf, A. P. *J. Med. Chem.* **1976**, *19*, 356.
(26) Musacchio, J. M.; Kopin, I. J.; Weise, V. K. *J. Pharmacol. Exp. Ther.* **1965**, *148*, 22.
(27) Firnau, G.; Sood, S.; Chirakal, R.; Nahmias, C.; Garnett, E. S. *J. Neurochem.* **1987**, *48*, 1077 and reference cited therein.
(28) Shore, P. A.; Busfield, D.; Alpers, H. A. *J. Pharmacol. Exp. Ther.* **1964**, *146*, 194.
(29) Cousineau, D.; Rose, C. P.; Goresky, C. A. *Circ. Res.* **1980**, *47*, 329.
(30) Tyce, G. M. *Am. J. Physiol.* **1978**, *235*, H289.
(31) (a) Rabinovitch, M. A.; Rose, C. P.; Rouleau, J. L.; Chartrand, C.; Wieland, D. M.; Lepanto, L.; Legault, F.; Suissa, S.; Rosenthall, L.; Burgeos, J. H. *Circ. Res.* **1987**, *61*, 797. (b) Minardo, J. D.; Tuli, M. M.; Mock, B. H.; Weiner, R. E.; Pride, H. P.; Wellman, H. N.; Zipes, D. P. *Circulation* **1988**, *78*, 1008. (c) Dae, M. W.; O'Connell, W.; Botvinick, E. H.; Ahearn, T.; Yee, E.; Huberty, J. P.; Mori, H.; Chin, M. C.; Hattner, R. S.; Herre, J. M.; Munoz, L. *Circulation* **1989**, *79*, 634.

bolic study to be published elsewhere,[32] the percent radioactivity as metabolites in the heart of guinea pig and dog was <0.3% at 1 h following intravenous injection of FMR. Metabolites of FMR, however, do appear in the blood, and the presence of these metabolites will require a correction in the blood activity curve used in kinetic modeling of the tracer.

The synthesis of FMR used in these studies is dependent on the primary generation of $[^{18}F]F_2$ from the nuclear reaction of neon-20 with deuterons. The subsequent reaction of $[^{18}F]F_2$ with sodium acetate produces $[^{18}F]AcOF$, which is used in the actual fluorination process.[33] However, in the generation of $[^{18}F]F_2$ from the neon target, carrier fluorine gas (ie. $[^{19}F]F_2$) must be present to allow recovery of atomic $[^{18}F]$fluorine from the nickel surface of the target.[15] As a consequence of the added carrier fluorine, the highest specific activities that we could achieve for FMR were approximately 10 Ci/mmol. A typical iv clinical dose of FMR (10 mCi/mmol) would be 5 mCi to a 70-kg patient, which would represent approximately 2.65 mg/kg of unlabeled FMR. In drug response studies in anesthetized dogs, blood pressure increases with unlabeled FMR have been observed in the 50–125 mg/kg range. This dose range is higher than the mass of unlabeled FMR likely to be administered in radiotracer scintigraphy studies. Nonetheless, the mass of unlabeled FMR in a 5-mCi dose is too close to pharmacological levels to be safely used in human subjects, especially in cardiac patients who might be highly susceptible to catecholamine-induced arrhythmias. Thus, before proceeding to clinical trials with FMR, a new radiosynthetic method must be developed which increases the specific activity of this promising neuronal mapping agent.

Experimental Section

Melting points were determined on a Mel-Temp apparatus and are uncorrected. ^1H NMR spectra were recorded on a Bruker 360-MHz spectrometer. IR spectra were recorded on a Perkin-Elmer 283B infrared spectrometer. Optical rotations were recorded on a Perkin-Elmer EM-241 polarimeter. Mass spectra were obtained on a Finnigan 4021 GCMS/DS (low resolution) or a UG70-250-S (high resolution) instrument.

Thin-layer chromatography was conducted on Analtech 0.25-mm glass plates precoated with silica gel GF. For flash column chromatography, E. Merck silica gel-60 (230–400 mesh) was used. Metaraminol [(–)-(*meta*-hydroxyphenyl)propanolamine] bitartrate salt was purchased from Sigma Chemical Co. 6-$[^{18}F]$Fluorometaraminol (FMR) was synthesized as described previously.[16] ^3H-Norepinephrine (14 Ci/mmol) was purchased from Du Pont/NEN. Custom tritiation of compounds **1** and **3** was performed by Midwest Research Institute, Kansas City, MO. C, H, and N analyses were performed by Spang Microanalytical Laboratory, Eagle Harbor, MI. Radio thin-layer chromatograms were obtained on a Berthold TLC linear analyzer LB 282 equipped with data acquisition system LB 500. HPLC was performed on a Waters liquid chromatograph equipped with a Radiomatic Flo-One radioactive flow detector and an ultraviolet detector (280 nm).

4-Iodometaraminol (1). A stirred solution of metaraminol bitartrate (1.0 g, 3.15 mmol) in 10 M NH_4OH (170 mL) was treated dropwise over a period of 45 min with a solution of I_2 (0.83 g, 3.27 mmol) in 95% EtOH (85 mL). The reaction was stirred in the dark under argon for 18 h and the solvent was removed in vacuo to afford a pale yellow oil. The crude product was treated with saturated brine (10 mL), extracted with EtOAc (4 × 100 mL), and the combined organic layers were dried with Na_2SO_4. The solvent was removed in vacuo and the residue was treated with an equivalent amount of D-tartaric acid (0.47 g, 3.15 mmol) and recrystallized from EtOH–Et_2O to afford white crystals: 0.48 g (34%); mp 159–160 °C dec; ^1H NMR of free base [$CDCl_3$ + CD_3OD (2 drops)] δ 7.63 (d, 1, J = 8.06 Hz, aromatic H_5), 6.82 (d, 1, J = 1.49 Hz, aromatic H_2), 6.54 (dd, 1, J = 1.72 Hz, J_2 = 8.07 Hz, aromatic H_6), 4.40 (d, 1, J = 4.98 Hz, C*H*OH), 3.06 (br s, 5, C*H*CH_3, NH_2, OH), 1.01 (d, 3, J = 6.51 Hz, CH_3); HRMS m/e 294.0002 ($C_9H_{13}NO_2I$ requires 293.9991); CIMS (methane) m/e (relative intensity) 294 (MH^+, 7), 276 (46), 151 (11), 133 (6), 123 (8), 105 (100), 94 (7), 87 (10), 77 (22), 76 (21).

6-Iodometaraminol (3). A solution of 6-(acetoxymercurio)-*N*-*t*-BOC-metaraminol (**2**,[16] 0.25 g, 0.48 mmol) in EtOAc (25 mL) was converted to the corresponding 6-chloromercurio derivative by treatment with saturated NaCl (25 mL) in a separatory funnel. The organic layer was removed and the aqueous layer was extracted further with EtOAc (25 mL), and the combined organic layers were dried over Na_2SO_4. Evaporation of the solvent under reduced pressure afforded a white solid which was used directly in the next step.

A stirred solution of the 6-chloromercurio derivative in $CHCl_3$ (10 mL) was treated with I_2 (0.12 g, 0.48 mmol) portionwise over a 20-min period and stirring was continued in the dark for 2 h. The solvent was removed under reduced pressure, the residue was treated with saturated brine (25 mL) and extracted with EtOAc (2×25 mL), and the combined organic layers were dried over Na_2SO_4. Removal of solvent in vacuo afforded 300 mg of the crude 6-iodo-*N*-*t*-BOC-metaraminol, which was treated with CH_3CN–6 N HCl (5:1) with stirring for 30 min at room temperature to remove the *t*-BOC protecting group. The solvent was removed and the residue was treated with EtOAc (2 × 100 mL) and dried over Na_2SO_4. Purification by flash chromatography on silica gel with $CHCl_3$–CH_3OH–NH_4OH (7:3:0.1) as eluant afforded 78 mg (56%) of pure material as determined by TLC on silica ($CHCl_3$–CH_3OH–NH_4OH, 7:3:0.1); the R_f of **3** was 0.31 and the R_f of metaraminol was 0.14. The product was crystallized as the bitartrate salt by treatment with an equivalent amount of D-tartaric acid (40 mg) in boiling CH_3OH (10 mL) for 5 min. Recrystallization from CH_3OH–Et_2O afforded a cream solid: mp 175–178 °C dec; ^1H NMR of free base [$CDCl_3$ + CD_3OD (2 drops)] δ 7.58 (d, 1, J = 8.50 Hz, aromatic H_5), 7.09 (d, 1, J = 2.94 Hz, aromatic H_2), 6.56 (dd, 1, J_1 = 3.02 Hz, J_2 = 8.50, aromatic H_4), 4.82 (d, 1, J = 3.3 Hz, C*H*OH), 3.40 (br s, s, C*H*CH_3, NH_2, OH), 1.03 (d, 3, J = 6.81 Hz, CH_3); HRMS m/e 294.0012 ($C_9H_{13}NO_2I$ requires 293.9991); CIMS (ammonia) m/e (relative intensity) 294 (MH^+, 100), 194 (4), 182 (3), 168 (24), 150 (4).

Synthesis of [4-^{3}H]Metaraminol. A sample of 19 mg (43 mmol) of 4-iodometaraminol D-tartrate dissolved in 5 mL of absolute ethanol was tritiated at room temperature with 10 Ci of tritium gas for 16 h at atmospheric pressure in the presence of 11.5 mg of 10% Pd/C. The tritium was handled with a Toepler pump and completion of the reaction was confirmed by the observed pressure drop. The reaction mixture was then evaporated in vacuo and labile tritium was removed by consecutive "chasing" in vacuo with 5 × 3 mL of methanol. The residue dissolved in methanol was filtered through a fritted-glass Büchner funnel packed with Celite and washed with 15 mL of dry methanol. Yield was 888 mCi of crude tritiated metaraminol with a radiochemical purity of 90% as determined by radio-TLC on silica gel using methanol–NH_4OH (98:2) as eluant (R_f = 0.15). Purification was accomplished by C-18 Sep-Pak chromatography using 0.2 M $NH_4H_2PO_4$–THF (85:15) as eluant. Final radiochemical purity of the ^3H tracers was >98%. Specific activity was 19.5 Ci/mmol.

Evidence for retention of configuration at the benzylic carbon was based on comparison of the UV/radio-HPLC behavior of the ^3H tracers with a mixture of *erythro*- and *threo*-metaraminol obtained by partially racemizing metaraminol in 6 N HCl at reflux.[17] A Beckman Ultrasphere IP column fitted with a guard column, 4.6 mm × (45 + 250 mm), was used under the following conditions: 50 mM sodium acetate (pH 4.75) and 10 mM sodium pentane sulfonate–methanol (75:25); flow rate of 1 mL/min and UV monitoring at 254 nM. Retention times of 10.3 and 11.4 min were observed for the erythro and threo isomers, respectively.

[^{125}I]Iodometaraminols. To a 5-mL thick-walled "V" vial containing 0.5 mL (1 mg/mL of H_2O) of metaraminol bitartrate and a spin vane was added 20 μL of 0.1 N NaOH solution containing 4.0 mCi of sodium [^{125}I]iodide followed by 20 μL of 0.3

(32) Rosenspire, K. C.; Gildersleeve, D. L.; Massin, C. C.; Mislankar, S. G.; Wieland, D. M. *Nucl. Med. Biol.* **1989**, *16*, 735.
(33) Jewett, D. M.; Potocki, J. F.; Ehrenkaufer, R. E. *J. Fluorine Chem.* **1984**, *24*, 477.

M potassium phosphate buffer (pH = 6.75). The reaction was initiated by the addition of 20 μL of an aqueous chloramine-T solution (0.34 mg/mL). The vial was closed with a Teflon-lined screw cap and the reaction mixture was stirred at ambient temperature for 5 min and then manually shaken for a few seconds. A 20-μL aliquot of aqueous $NaHSO_3$ solution (1.4 mg/mL) in a microliter syringe was added to quench the reaction and the solution was stirred for an additional 5 min. Radio-TLC on silica gel (EtOH–EtOAc–NH_4OH 20:20:1) showed that the reaction had proceeded to the extent of ~99%. The solution was passed through an anion-exchange column (Cellex-D, OH form) under partial vacuum in a closed system to remove residual traces of free [^{125}I]iodide. Further elution with 0.005 M sodium acetate buffer (3 × 1 mL) provided 3.36 mCi (82%) of crude radioactive product. HPLC analysis of the radioiodinated mixture was performed on a Waters μ Bondapak C-18 column (3.9 × 300 mm) using 0.2 M $NH_4H_2PO_4$–THF (85:15) as eluant at 2 mL/min. Three major radioactive compounds eluted with retention times of 3.4, 5.6, and 12.9 min; the peaks represented 12.6%, 13.5%, and 71.8%, of the total radioactivity, respectively. The second and third radioactive peaks coeluted with authentic 6-iodometaraminol and 4-iodometaraminol, respectively. The ^{125}I isomers were purified either by chromatography using a C-18 Sep-Pak with a gradient of aqueous NH_4OAc–EtOH or by reversed-phase HPLC on a Phenomenex Ultramex C-18 column (4.6 × 150 mm) with NH_4OAc–EtOH (9:1) as eluant at 2 mL/min. Radiochemical purity of both tracers was 95–98% as determined by radio-HPLC utilizing the analytical system described above.

Tissue Distribution Studies. 1. ^{3}H- and ^{125}I-Labeled Tracers. These studies, results of which are shown in Tables I and III, were performed in female mongrel dogs (13.3–19.7 kg). For each time interval evaluated, one to three dogs received bolus cephalic vein injections of tracer in 2.0 mL of sterile acetate buffer (pH 4.5). Animals were administered 92–100 μCi of ^{3}H tracer; injections of 75 and 55 μCi were utilized in the 4-[^{125}I]iodometaraminol and 6-[^{125}I]iodometaraminol experiments, respectively. The dogs were sacrificed 30 min or 24 h later by rapid iv injection of sodium pentobarbital. Duplicate tissue samples of major organs were removed for analysis. The weighed tissue samples from the ^{3}H tracer studies were oxidized in a Packard 306 Tri-Carb sample oxidizer and then counted in a Packard 3330 liquid-scintillation counter with corrections made for background and counter efficiency.

2. 6-[^{18}F]Fluorometaraminol (FMR). These studies (Figure 1; Table IV) were performed on 20 Sprague–Dawley rats (Charles River Breeding Laboratories, Inc., Wilmington, MA) weighing 182–335 g and in two male mongrel dogs (20.1 and 20.4 kg) and two female mongrel dogs (15.0 and 18.6 kg). Rats received bolus injections of FMR (25 or 50 μCi) via the femoral vein under ether anesthesia. Tracer was dissolved in 0.20–0.30 mL of sterile 0.15 M acetate buffer, pH 4.5. Dogs received bolus injections of FMR through the cephalic vein, 2.0 mCi (males) or 0.45 mCi (females), in 2.0 mL of sterile 0.15 M acetate buffer, pH 4.5. Rats were killed by decapitation at various times following tracer injection; dogs were sacrificed 1 h after tracer injection by rapid iv injection of sodium pentobarbital. Tissue samples of each major organ were excised, washed free of blood with 0.9% saline solution, blotted dry, and quickly weighed and counted on a Packard 5780 autogramma counter for 1 min. The method for isolating adrenomedullary tissue has been described previously.[34] To normalize for differences in animal weights, tissue concentrations are expressed either as dose/g normalized to a 200 g rat or, in the case of dogs, as percent kilogram dose per gram (% kg dose/g). Concentrations are decay corrected.

PET Imaging Studies. Thoracotomies were performed on five dogs; an area of the anterior wall of the left ventricle was then painted with a thin layer of phenol using a cotton-tipped applicator. Anesthesia was induced with 5% Surital solution (0.45 mL/kg) and maintained during surgery by halothane inhalation (4% initially; 0.5–2% for maintenance). This procedure and subsequent imaging studies were done in accordance with institutional guidelines. The left anterior descending artery (LAD) was bisected by a circle of 88% phenol (v/v) in ethanol in four of five dogs (Figure 5). Thoracotomies without phenol application were also performed on three control dogs in which normal saline was applied to the surface of the anterior wall of the left ventricle. The chests were surgically closed and all animals recovered for 4–7 days prior to tracer studies. The general procedure has been described in more detail.[3]

Cross-sectional tomographic heart images were obtained with dogs in the supine position under pentobarbital anesthesia (30 mg/kg iv). Imaging was performed with a TCC 4600 A tomograph which has a resolution of 1.1 × 1.1 × 0.95 cm. Five planes with center-to-center spacing of 1.15 cm were scanned simultaneously. [^{13}N]NH_3 or FMR was injected iv and dynamic PET images were obtained to define uptake and clearance kinetics in heart. The two tracer injections were made through indwelling catheters in the saphenous veins of opposite legs. The dogs were fitted with tracheal breathing tubes. Body temperature was maintained with a heat lamp. Heart rate, blood pressure, respiration rate, and body temperature were monitored throughout the study.

Pharmacological Blocking Studies. The extent to which FMR, [^{3}H]norepinephrine, [^{3}H]metaraminol, and thallium-201 localize in the sympathetic nerves of the heart in vivo was determined (Table II; Figures 3 and 4) by measuring the decrease in tracer concentration in the rat heart following pretreatment with drugs or neurotoxins known to either selectively block entry/storage of norepinephrine in the neuron or selectively destroy the nerve endings. Female Sprague–Dawley rats weighing 200–300 g were administered the following agents under ether anesthesia: desipramine hydrochloride (Revlon Care Group, Tuckahoe, NY), 10 mg/kg ip, 30 min prior to tracer injection; reserpine (Sigma Chemical Co., St. Louis, MO), 1 mg/kg ip, 3 h prior to tracer injection; 6-hydroxydopamine hydrobromide (Aldrich Chemical Co., Milwaukee, WI), 100 mg/kg ip, 5 days prior to tracer injection. Control animals received equal volume injections of vehicle. Animals were then injected iv (femoral vein) with FMR (5–10 μCi), [^{3}H]norepinephrine (25 μCi), [^{3}H]metaraminol (15 μCi), or thallium-201 (23–28 μCi) and sacrificed by decapitation 90 min later. Tissue radioactivity levels were determined in selected tissues as described under Tissue Distribution Studies. The drug doses and timing of the subsequent tracer injections were based on best estimates obtained from literature reports;[36] parallel studies with [^{3}H]norepinephrine also confirmed the effectiveness of the drug treatments.[16] Solutions of 6-hydroxydopamine were freshly prepared in physiological saline just prior to injection to avoid air oxidation.

Statistical Analysis. Data are expressed as mean ± SD or mean ± SEM. Significance was determined using the Student's *t* test.

Acknowledgment. We thank the staff of the University of Michigan PET Facility for their assistance in carrying out the PET studies, James W. Crudup and the Animal Surgery Operating Room of the University of Michigan Department of Surgery for performing the dog surgery and phenol painting, the University of Michigan Diabetes Research and Training Center for HPLC analyses of NE, and Linder Markham for typing the manuscript. We also thank James C. Sisson and W. Les Rogers for critically reviewing the manuscript and Richard J. Flanagan for helpful suggestions on the organomercury aspects of the chemistry. This work was funded by NIH Grant HL27555.

Registry No. 1, 124201-36-1; **2**, 112138-38-2; **3**, 124201-38-3; 6-fluorometaraminol, 112113-60-7; metaraminol, 54-49-9; 4-

(34) Wieland, D. M.; Mangner, T. J.; Inbasekaran, M. N.; Brown, L. E.; Wu, J-L. *J. Med. Chem.* **1984**, *27*, 149.
(35) Sisson, J. C.; Wieland, D. M.; Sherman, P.; Mangner, T. J.; Tobes, M. C.; Jaques, S., Jr. *J. Nucl. Med.* **1987**, *28*, 1620.
(36) (a) Axelrod, J. G.; Herttling, G.; Potter, L. *Nature (London)* **1962**, *194*, 297. (b) Daly, J. W.; Creveling, C. R.; Witkop, B. *J. Med. Chem.* **1966**, *9*, 280. (c) DeChamplain, J.; Nadeau, R. *Fed. Proc., Fed. Am. Soc. Exp. Biol.* **1971**, *30*, 877. (d) Maxwell, R. A.; Ferris, R. M.; Burcsu, J. E. In *The Mechanisms of Neuronal and Extraneuronal Transport of Catecholamines*; Paton, D. M., Ed.; Raven: New York, 1976, p 95.

[^{3}H]metaraminol, 124201-39-4; 6-[^{18}F]fluorometaraminol, 112113-61-8; 6-[^{3}H]metaraminol, 124201-40-7; metaraminol bitartrate, 33402-03-8; 6-[^{125}I]iodometaraminol, 124201-41-8; 4-[^{125}I]iodometaraminol, 124201-42-9.

Supplementary Material Available: Tissue distribution data in rats for the 4- and 6-[^{125}I]iodometaraminols and the [4-^{3}H]- and [6-^{3}H]metaraminols are available (2 pages). Ordering information is given on any current masthead page.

Small Peptide Inhibitors of Smooth Muscle Myosin Light Chain Kinase[1]

Federico C. A. Gaeta,*,† Laura S. Lehman de Gaeta,*,‡ Timothy P. Kogan, Yat-Sun Or, Carolyn Foster, and Michael Czarniecki*,[2]

Departments of Chemical Research and Pharmacology, Schering-Plough Research, 60 Orange Street, Bloomfield, New Jersey 07003. *Received July 5, 1989*

The pentapeptide Ser-Asn-Val-Phe-Ala-OBzl has been identified as the smallest inhibitory peptide of myosin light chain kinase (MLCK) derived from the primary sequence of the light chain phosphorylation site. The specific contributions of individual amino acid side chains and backbone elements of this pentapeptide toward the stabilization of the enzyme–inhibitor (E·I) complex have been evaluated. The potency of these peptides as inhibitors of MLCK has been enhanced by the incorporation of synthetic nonnatural amino acids into the sequence. Finally, it has been demonstrated that these peptide sequences could be converted into pseudopeptides with synthetic nonpeptide subunits designed to mimic peptide bonds, and that certain pseudopeptides retained the high-affinity inhibition of the parent pentapeptides.

Myosin light chain kinase (MLCK) is a Ca^{2+}-calmodulin dependent enzyme, which catalyzes the transfer of the γ-phosphate group of ATP to a Ser[19] residue in the 20 kDa phosphorylatable light chains of myosin (MLC). In smooth muscle, phosphorylation of Ser[19] is a prerequisite for stimulation of myosin ATPase activity and cross-bridge cycling leading to muscle contraction.[3] Thus, specific inhibitors of smooth muscle MLCK are expected to be smooth muscle relaxants, and may be useful as novel therapeutic agents in the treatment of disease states such as hypertension and bronchoconstriction.

Kemp and co-workers have shown that small polybasic peptide fragments from the amino terminus of MLC are effective substrates for the phosphorylation reaction.[4,5] Further, they demonstrated that a critical spatial requirement exists between the phosphorylatable serine and an assembly of basic residues near the N terminus. The smallest peptide that retained substrate characteristics comparable to those of native light chains was the tridecapeptide 1. Shorter peptides such as **2**, which lack the

	11 12 13 14 15 16 17 18 19 20 21 22 23
MLC_{11-23}	-Lys-Lys-Arg-Pro-Gln-Arg-Ala·Thr-Ser*-Asn·Val·Phe-Ala-
1	Lys-Lys-Arg-Pro-Gln-Arg-Ala·Thr-Ser*-Asn-Val-Phe-Ser-NH_2
2	Arg·Ala·Thr-Ser*-Asn-Val-Phe·Ser-NH_2
3	Lys-Lys-Arg-Ala·Ala·Arg-Ala·Thr-Ser*-NH_2
4	Lys·Lys-Arg-Ala-Ala-Arg-NH_2
5	Lys-Lys·Arg-Ala-Ala·Arg·Ala·Thr-Ser*·Asn·Val-Phe-NH_2
6	Lys-Lys-Arg·Ala-Ala·Arg-Ala-Thr-Ser*·Asn·Ala-Ala-NH_2

*phosphorylatable serine

critical cluster of basic residues, manifest a modestly smaller V_{max} but markedly increased $(K_m)_{app}$ values. Interestingly, smaller peptides such as **3** which contain the cationic cluster but lacked residues beyond the phosphorylatable serine were also poor substrates.[6] This effect resulted almost exclusively from a lower V_{max}.

Small peptides such as **3** have $(K_m)_{app}$ that are essentially identical with those of native myosin light chains (MLC), essentially making these inhibitors of the enzyme rather than substrates. These peptides were good inhibitors of MLCK, in the low micromolar range. Recently, hexapeptide **4** was determined to be the minimal inhibitory peptide containing these basic residues.[7]

We[8] and others[9] have demonstrated that polybasic peptide fragments derived from the primary sequence of chicken gizzard MLCK also were very potent inhibitors. Recent evidence suggests that this region of the enzyme is involved in pseudosubstrate autoregulation. These peptides are derived from a region of the kinase probably involved in calmodulin binding and the mechanism by which they inhibit the enzyme appears to be complex. Inhibition occurs not only by binding calmodulin but also by competition of these peptides with MLC for the active site of the enzyme.

MLCK is a Ca^{2+}-calmodulin-dependent kinase, thus it is expected that calmodulin antagonists will be inhibitors. Compounds such as W-7 have been shown to inhibit the enzyme.[10,11] Finally, myosin light chain kinase can be inhibited by an active site mechanism with small nonpeptides which compete with the ATP cosubstrate at the catalytic site. Within this class of inhibitors is 5′-chloro-5′-deoxyadenosine[12] as well as the arylsulfonamide kinase

† Present address: Cytel Corp., 11099 N. Torrey Pines Road, La Jolla, CA 92037.

‡ Present address: Amylin Corp. 12520 High Bluff Drive, San Diego, CA 92130.

(1) Presented in part at The Third Chemical Congress of North America, Toronto, Canada, June 1988 and *FASEB J.* **1988**, *2*, A332.
(2) Address for correspondence to this author: Schering-Plough Research, 60 Orange Street, Bloomfield, NJ 07003.
(3) (a) Kamm, K. E.; Stull, J. T. *Annu. Rev. Pharmacol. Toxicol.* **1985**, *25*, 593. (b) Itoh, T.; Ikebe, M.; Kargacin, G. J.; Hartshorne, D. J.; Kemp, B. E.; Fay, F. S. *Nature* **1989**, *338*, 164.
(4) Kemp, B. E.; Pearson, R. B. *J. Biol. Chem.* **1985**, *260*, 3355.
(5) Kemp, B. E.; Pearson, R. B.; House, C. *Proc. Natl. Acad. Sci. U.S.A.* **1983**, *80*, 7471.
(6) Pearson, R. B.; Misconi, L. Y.; Kemp, B. E. *J. Biol. Chem.* **1986**, *261*, 25.
(7) Hunt, J. T.; Floyd, D. M.; Lee, V. G.; Little, D. K.; Moreland, S. *Biochem. J.* **1989**, *257*, 73.
(8) Gaeta, F. C. A.; Foster, C. F., manuscript in preparation.
(9) (a) Kemp, B. E.; Pearson, R. B.; Guerriero, V., Jr.; Bagchi, I. C.; Means, A. R. *J. Biol. Chem.* **1987**, *262*, 2542. (b) Pearson, R. B.; Wettenhall, R. E. H.; Means, A. R.; Hartshorne, D. J.; Kemp, B. E. *Science* **1988**, *241*, 970.
(10) Zimmer, M.; Hofmann, F. *Eur. J. Biochem.* **1984**, *142*, 393.
(11) The antidepressent trifluoperazine has been shown to inhibit smooth muscle MLCK by a mixed mechanism which involves an unknown component in addition to the calmodulin binding. Silver, P. J.; Sigg, E. B.; Moyer, J. A. *Eur. J. Pharmacol.* **1986**, *121*, 65.

0022-2623/90/1833-0964$02.50/0